ISSN 1070-3284, Russian Journal of Coordination Chemistry, 2018, Vol. 44, No. 12, pp. 755–764. © Pleiades Publishing, Ltd., 2018.
Original Russian Text © I.I. Dyukova, T.A. Kuz'menko, V.Yu. Komarov, T.S. Sukhikh, E.V. Vorontsova, L.G. Lavrenova, 2018, published in Koordinatsionnaya Khimiya, 2018, Vol. 44, No. 6, pp. 393–401.

Coordination Compounds of Cobalt(II), Nickel(II), and Copper(II) Halides with 2-Methyl-1,2,4-Triazolo[1,5-a]benzimidazole

I. I. Dyukova[a, b, *], T. A. Kuz'menko[c], V. Yu. Komarov[a, b], T. S. Sukhikh[a, b], E. V. Vorontsova[d], and L. G. Lavrenova[a, b, **]

[a] *Nikolaev Institute of Inorganic Chemistry, Siberian Branch, Russian Academy of Sciences, Novosibirsk, 630090 Russia*

[b] *Novosibirsk National State Research University, Novosibirsk, 630090 Russia*

[c] *Institute of Physical and Organic Chemistry, Southern Federal University, Rostov-on-Don, Russia*

[d] *Institute of Molecular Biology and Biophysics, Federal Research Center of Fundamental and Translational Medicine, Novosibirsk, Russia*

**e-mail: ira.dukova.94@mail.ru*

***e-mail: ludm@niic.nsc.ru*

Received February 22, 2018

Abstract—New coordination compounds of Co(II), Ni(II), and Cu(II) halides with 2-methyl-1,2,4-triazolo[1,5-a]benzimidazole (L), $[Co(L)_2Cl_2]$ (**Ia**), $[Ni(L)_2(H_2O)_4]Cl_2 \cdot 4H_2O$ (**II**), and $[Cu_2(L)_4(\mu\text{-}Br)_2Br_2]$ (**IIIa**), are synthesized. The complexes are studied by X-ray structure analysis (CIF files CCDC nos. 1825006–1825008), electronic (diffuse reflectance) spectroscopy, and IR spectroscopy. In compounds **Ia**, **II**, and **IIIa**, ligand L is coordinated to the metal by the N^4 atom of the triazole fragment. The study of the cytotoxic effect of the ligand and synthesized complexes on the Hep-2 line (laryngeal cancer cells) shows a considerably higher activity of the copper(II) complex than that of the ligand.

Keywords: synthesis, complexes, 3*d* metals, 2-methyl-1,2,4-triazolo[1,5-a]benzimidazole, X-ray structure analysis, electronic spectroscopy, IR spectroscopy, cytotoxic activity

DOI: 10.1134/S107032841812014X

INTRODUCTION

Polynitrogen heterocyclic compounds represent a promising class of ligands for the synthesis of transition metal complexes with nontrivial magnetic properties and biological activity. The diversity of possible coordination modes of these ligands to the metal enables one to obtain complexes with different structures and, as a consequence, with various physicochemical and biological properties. Benzimidazole and its derivatives exhibiting a wide range of pharmacological properties form a promising class of compounds for the synthesis and study of the complexes. These compounds can exert antibacterial, antiparasitic, anti-inflammatory, antiviral, and antitumor effects [1–6]. In addition, a moderate anti-AIDS effect was found for benzimidazole [7]. It is known that sometimes the complex formation of biologically important organic compounds with metal ions makes it possible to considerably enhance their efficiency compared to that of the free organic ligand [8–11]. Owing to this, coordination compounds are widely studied as potent biologically active substances. The cytotoxic effect of the Pt(II) and Pd(II) complexes with 2-aminomethylbenzimidazole (L^1) of the general composition $[M(L^1)Cl_2]$ was studied [12]. Both complexes exhibit a high antitumor activity toward various cell lines. The complexes of the metals of the first transition series (Co(II), Ni(II), Cu(II), and Zn(II)) with 2-(4'-thiazole)benzimidazole (thiabendazole) and other benzimidazole derivatives manifest a pronounced antimicrobial activity [13, 14]. The results of studying the cytotoxicity of the heteroligand Cu(II) complexes containing thiabendazole or 2-(2-pyridyl)benzimidazole and benzoic acid were described [15]. These compounds exhibit a high antitumor activity and are promising for further investigations. Thus, an analysis of literature data shows that the transition metal complexes with benzimidazole and its derivatives manifest biological activity in a wide range.

Fused systems based on benzimidazole in which the second azole cycle is added to the 1–2 bond of the benzimidazole molecule attract considerable attention of researchers [16, 17]. These compounds are characterized by a complicated mutual influence of fused rings, which is necessary to study for the development of heterocycle chemistry. In addition, fused systems, in particular, imidazo[1,2-a]benzimidazoles have a pronounced biological activity [18, 19]. A promising

class of these compounds is formed by 1,2,4-triazolo[1,5-a]benzimidazoles, whose coordination compounds can manifest both magnetic and biological activities. 1,2,4-Triazoles as ligands are coordinated to 3*d*-metal ions predominantly via the bidentate bridging mode due to which the obtained compounds with the oligo- or polynuclear structure have a pronounced magnetic activity [20–22]. A series of 2,4-dihydro-3*H*-1,2,4-triazole-3-thione compounds is shown [23, 24] to possess the antidepressant properties and anticonvulsant activity. The 1,2,4-triazole derivatives manifest a significant antioxidant activity [25]. A considerable antitumor activity compared with the effect of cisplatin was found for the Pt(II) complex with 3,5-diacetyl-1,2,4-triazolebis(4,4-dimethylthiosemicarbazone) (L^2) of the composition $[Pt(\mu\text{-}L^2)]_2$ [26]. In addition, the Ru(III) complexes with the ligands bearing the 1,2,4-triazole fragment are promising antitumor drugs alternative to the Pt(II)-based drugs [27]. The study of the antibacterial and fungicidal activities of the Co(II), Ni(II), and Cu(II) complexes with the 1,2,4-triazole-containing Schiff bases toward several species of bacteria and fungi was reported [28].

It seemed reasonable to synthesize new coordination compounds of cobalt(II), nickel(II), and copper(II) with 2-methyl-1,2,4-triazolo[1,5-a]benzimidazole (L) and to study their structures and cytotoxic effect.

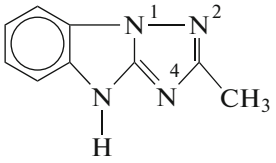

(L)

EXPERIMENTAL

The following reagents were used in the syntheses: $CoCl_2 \cdot 6H_2O$, $NiCl_2 \cdot 6H_2O$, and $CuBr_2$ (analytical grade), ligand L synthesized according to a known procedure [17], and ethanol (rectificate).

Synthesis of complexes $Co(L)_2Cl_2 \cdot 0.5H_2O$ (I), $[Ni(L)_2(H_2O)_4]Cl_2 \cdot 4H_2O$ (II), and $Cu(L)_2Br_2$ (III). A weighed sample of ligand L (0.34 g, 2 mmol) was dissolved in ethanol (7 mL) on heating in a water bath, and a hot solution of the corresponding metal salt (1 mmol; 0.24 g of $CoCl_2 \cdot 6H_2O$ and $NiCl_2 \cdot 6H_2O$, or 0.22 g of $CuBr_2$) in ethanol (3 mL) was added with stirring. The obtained solutions were evaporated to ~1/3 of the initial volume. Finely crystalline bright blue $Co(L)_2Cl_2 \cdot 0.5H_2O$ or gray-brown $Cu(L)_2Br_2$ precipitated from the mother liquors on gradual cooling to room temperature. The precipitates were filtered off, washed with ethanol several times, and dried in air. The yields were 76 and 31% for complexes **I** and **III**, respectively. The data of elemental and X-ray diffraction analyses showed that the isolated polycrystalline precipitate contained a mixture of phases of different compositions for complex **II**. Owing to this the further studies for the nickel-containing complex were conducted only with the coarsely crystalline phase of **II** isolated from the mother liquor. The crystals suitable for X-ray structure analysis of the compositions $[Co(L)_2Cl_2]$ (**Ia**), **II**, and $[Cu_2(L)_4(\mu\text{-}Br)_2Br_2]$ (**IIIa**) precipitated from the mother liquors of compounds **I**–**III**, respectively, on prolonged storage at room temperature up to the complete removal of the solvent.

For $C_{18}H_{17}N_8O_{0.5}Cl_2Co$ (**I**)			
Anal. calcd., %	C, 44.7	H, 3.5	N, 23.2
Found, %:	C, 44.5	H, 3.4	N, 23.3
For $C_{18}H_{32}N_8O_8Cl_2Ni$ (**II**)			
Anal. calcd., %	C, 35.0	H, 5.2	N, 18.1
Found, %	C, 35.1	H, 4.8	N, 19.4
For $C_{36}H_{32}N_{16}Br_4Cu_2$ (**III**)			
Anal. calcd., %	C, 38.1	H, 2.8	N, 19.7
Found, %	C, 37.2	H, 2.7	N, 19.5

Elemental analyses of the complexes were conducted on a EURO EA 3000 instrument (EuroVector, Italy) at the Analytical Laboratory of the Nikolaev Institute of Inorganic Chemistry (Siberian Branch, Russian Academy of Sciences).

The X-ray diffraction analyses of the polycrystalline samples were carried out on a Shimadzu XRD 7000 diffractometer (CuK_α radiation, Ni filter, scintillation detector) at room temperature. The samples were triturated in heptane and deposited on the polished side of a quartz cell. The recording was carried out in an angle range of 5°–60° with an increment of 0.03° and an exposure of 1 s. The positions of the observed reflections in the range $2\theta = 5°–20°$ are presented in Table 1. The qualitative analysis of the diffraction patterns was performed by comparing with the theoretical diffraction patterns calculated for the structures of the complexes isolated from compounds **Ia**, **II**, and **IIIa** (described in the present article), free ligand (deposited with the Cambridge Crystallographic Data Centre, CIF file CCDC no. 1825031 [29]), and inorganic salts and their hydrates, which can be formed under these conditions (deposited with the Inorganic Crystal Structure Database, ICSD nos. 69393, 20280, 69392, 43728, 280139, 20279, 22284, 22079, and 67555 [30]).

X-ray structure analysis was conducted using a standard procedure on automated four-circle Bruker-Nonius X8 APEX (for complex **Ia**) and Bruker DUO APEX (for complexes **II** and **IIIa**) diffractometers (graphite monochromator, two-coordinate 4KCCD detectors). The main crystallographic data and refinement details are presented in Table 2. The diffraction data were measured using the MoK_α radiation (λ =

Table 1. X-ray diffraction data (2θ, deg) for the samples of compounds **I**, **II**, and **III***

Complex	2θ, deg
I	**7.28** s, 8.74 w, 10.00 w, **11.54** m, 12.78 m, **13.98** w, **14.56** m, **15.46** w
II	6.47 vs, **8.76** s, **10.04** m, 10.96 m, 11.66 w, 12.77 m, **13.15** w sh, **13.41** m, **15.27** w, **15.89** m, **17.13** m, **17.59** w, **18.31** m, **19.54** s
III	**6.56** m, 6.78 w sh, 6.90 m, **9.34** m, **10.89** m, **11.18** w sh, **11.43** s, 11.57 w sh, 17.66 m, 19.8 m

* Reflections corresponding to the phases characterized by X-ray structure analysis are given by bold.

0.71073 Å). An absorption correction was applied empirically (by equivalent reflection intensities) (SADABS) [31]. The structures were solved by a direct method and refined by full-matrix least squares for F^2 in the anisotropic approximation for all non-hydrogen atoms (SHELXTL [32] and OLEX2 graphical shell [33]). The hydrogen atoms of ligand L were localized geometrically and refined by the riding model. The hydrogen atoms of the water molecules were localized from the difference Fourier synthesis and refined in the isotropic approximation with fixed values of $U_{iso}(H) = 1.5U_{eq}(O)$. The coordinates of atoms and thermal parameters for compounds **Ia**, **II**, and **IIIa** were deposited with the Cambridge Structural Database [29] (CSD nos. 1825006–1825008; http://www.ccdc.cam.ac.uk/data_request/cif).

IR absorption spectra were recorded on a Scimitar FTS 2000 spectrometer in the range 400–4000 cm^{-1}. The samples were prepared as suspensions in Nujol and in the fluorinated oil. The Kubelka–Munk diffuse reflectance spectra were detected on a UV-3101 PC scanning spectrophotometer (Shimadzu) at room temperature.

The cytotoxic effects of the ligands and complexes were studied for the human line of the laryngeal cancer cells (Hep-2) using the double-staining procedure with Hoechst 33342 and Propidium Iodide [34]. The vital activity of the cell culture was maintained in the medium Dulbecco's Minimum Essential Medium (DMEM) with the 10% content of fetal bovine serum (FBS, HyClone) in a wetted atmosphere with the 5% content of CO_2 at 37°C. The cells (5×10^3) were distributed in a 96-well tray (Corning) in 100 μL of the medium in each well and were incubated overnight.

Then the cell culture was treated with the studied compounds in concentrations of 0.2, 1, 5, 25, and 125 μM for 48 h. Ethanol or a 50% water–ethanol solution was used for the preparation of solutions of the ligands and complexes. Then two types of the fluorescent dyes Hoechst 33342 (exposure for 30 min at 37°C) and Propidium Iodide (exposure for 10 min at 37°C) were added to the treated and control cells. Detection was conducted in the automated regime (four fields per well) on an IN Cell Analyzer 2200 instrument (GE Healthcare, UK). The results were presented as the percentage content of living, dead, and apoptosis cells.

RESULTS AND DISCUSSION

The complexes of cobalt(II) and nickel(II) chlorides, as well as copper(II) bromide, with ligand L were isolated from ethanol solutions at the molar ratio M : L = 1 : 2.

All studied polycrystalline samples contain the phases, whose structures were determined by X-ray structure analysis. The samples of complexes **I** and **III** are strongly textured, which is observed as the characteristic deviation of the basal reflection intensities from the calculated values. No reflections from the initial phases and no known products of their solvation are observed in all samples studied. Sample **Ia** contains only a minor amount of another phase in addition to $[Co(L)_2Cl_2]$, whereas sample **III** contains a comparable amount of another phase with a close composition together with the phase $[Cu_2(L)_4(\mu\text{-}Br)_2Br_2]$. Taking into account the CHN analysis data, we can assume that the additional phases have the ratio M : L = 1 : 2 and differ by the content of solvate water only. These phases will be studied in detail elsewhere.

According to the data of X-ray structure analysis, molecular compound **Ia** contains two crystallographically nonequivalent Co atoms (Fig. 1). Two Cl^- ligands and two N atoms of ligands L are coordinated to each Co atom to form distorted tetrahedral coordination modes of the central atoms. In each molecule, the Co and Cl atoms exist in the partial positions 2*a* and 2*b* (Wyckoff notation) with the symmetry *m* and ligands L in general positions are equivalent in pairs. On the whole, the geometries of both molecules are nearly identical, and the differences in bond lengths do not exceed 0.03 Å. The Co–N and Co–Cl distances lie in the expected range according to the CSD [29].

Unlike complex **Ia**, complex **II** is cationic (Fig. 2). The coordination sites at the central atom in complex **II** are occupied by four H_2O ligands and two N atoms of two ligands L; i.e., Ni exists in the octahedral environment, which is characteristic of this atom. The complex is centrosymmetric, and the Ni atom lies in the partial position 4*a*. According to the CSD, the Ni–N and Ni–O distances in complex **II** are in the expected range.

Compound **IIIa** is a binuclear molecular centrosymmetric complex (the position of the center of the molecule is 2*d*) in which the Cu atoms are linked

Table 2. Crystallographic data and structure refinement results for compounds **Ia**, **II**, and **IIIa**

Parameter	Value		
	Ia	**II**	**IIIa**
Empirical formula	$C_{18}H_{16}N_8Cl_2Co$	$C_{18}H_{32}N_8O_8Cl_2Ni$	$C_{36}H_{32}N_{16}Br_4Cu_2$
FW	474.22	618.12	1135.49
Crystal system	Orthorhombic	Orthorhombic	Monoclinic
Space group	$Pmc2_1$	$Pbca$	$P2_1/c$
a, Å	24.0517(9)	18.0527(8)	13.180(4)
b, Å	7.9917(3)	7.5651(3)	7.609(2)
c, Å	10.1646(3)	20.1655(9)	19.611(4)
β, deg	90	90	92.337(10)
V, Å^3	1953.78(12)	2754.0(2)	1965.1(9)
Z	4	4	2
ρ_{calcd}, g/cm^3	1.612	1.491	1.919
μ, mm^{-1}	1.175	0.954	5.202
F(000)	964.0	1288.0	1116.0
Crystal size, mm	0.45 × 0.1 × 0.1	0.22 × 0.15 × 0.06	0.29 × 0.04 × 0.04
Range of data collection over 2θ, deg	1.694–57.418	4.040–0.336	5.080–51.358
Ranges of indices h, k, l	$-20 \le h \le 32$ $-10 \le k \le 10$ $-9 \le l \le 13$	$-21 \le h \le 21$ $-8 \le k \le 9$ $-20 \le l \le 24$	$-16 \le h \le 16$ $-9 \le k \le 7$ $-23 \le l \le 19$
Number of measured reflections	10352	27511	13022
Number of independent reflections (R_{int})	4244 (0.0221)	2438 (0.0280)	3724 (0.0546)
R_σ	0.0470	0.0128	0.0585
Number of refined parameters	273	202	264
GOOF for F^2	1.121	1.069	1.011
R factor ($I > 2\sigma(I)$)	$R_1 = 0.0383$, $wR_2 = 0.0970$	$R_1 = 0.0245$, $wR_2 = 0.0611$	$R_1 = 0.0397$, $wR_2 = 0.0918$
R factor (all data)	$R_1 = 0.0412$, $wR_2 = 0.1011$	$R_1 = 0.0302$, $wR_2 = 0.0648$	$R_1 = 0.0636$, $wR_2 = 0.1010$
$\Delta\rho_{max}/\Delta\rho_{min}$, e Å^{-3}	2.68/–0.60	0.51/–0.43	0.58/–1.11

by two bridging bromide ions. The central atoms are also coordinated by one terminal Br^- ion and two N atoms of two ligands L (Fig. 3), as well as by two bridging bromide ions. Thus, the coordination number of Cu is 5. Since the central atom and three bromide ions bound to the central atom lie in one plane and the NCuN angle is 167.6°, the geometry of the coordination mode is closer to a trigonal bipyramid. However, the Br(1)CuBr(1') and Br(2)CuBr(1') angles differ substantially from 120° (Tables 3, 4). The Cu–(μ-Br) distances differ substantially, due to which the geometry of the $\{Cu_2(\mu\text{-}Br)_2\}$ fragment deviates noticeably from the orthorhombic one. This deviation is characteristic of the structures of the complexes of Cu in a similar environment and is observed in ~210 cases of 250 (CSD) [29]). The $\{Cu_2(Hal)_4\}$ fragment (Hal = Cl, Br) with the coordination number of Cu of 5 was considered.

In all three complexes, ligand L is coordinated to the metal by the atom of the N^4 type of the triazole fragment (see scheme for L). The geometries of ligand L in the discussed compounds are almost identical, and the differences in bond lengths do not exceed 0.02 Å. The structures of complexes **Ia** and **IIIa** exhibit different (in value) deviations of the geometry of the ligand from the planar one. The consideration of the deviation of the atoms of the ligand from the root-mean-square plane of the diazole ring $\{C_3N_2\}$ shows that the maximum deviation is observed for the atoms of the triazole rings $\{C_2N_3\}$ (Table 5). Since the cycles $\{C_6\}$ and $\{C_2N_3\}$ lie at one side from the $\{C_3N_2\}$ plane, this deviation cannot be explained by disorder-

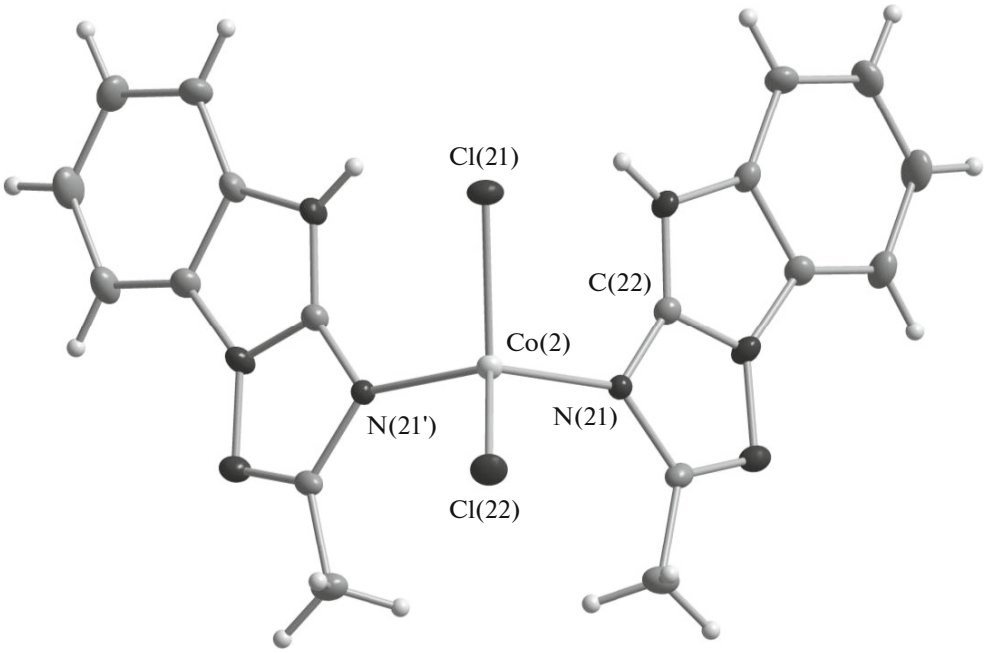

Fig. 1. Structure of complex $[Co(L)_2Cl_2]$ (**Ia**). Atomic shift ellipsoids are presented with 50% probability.

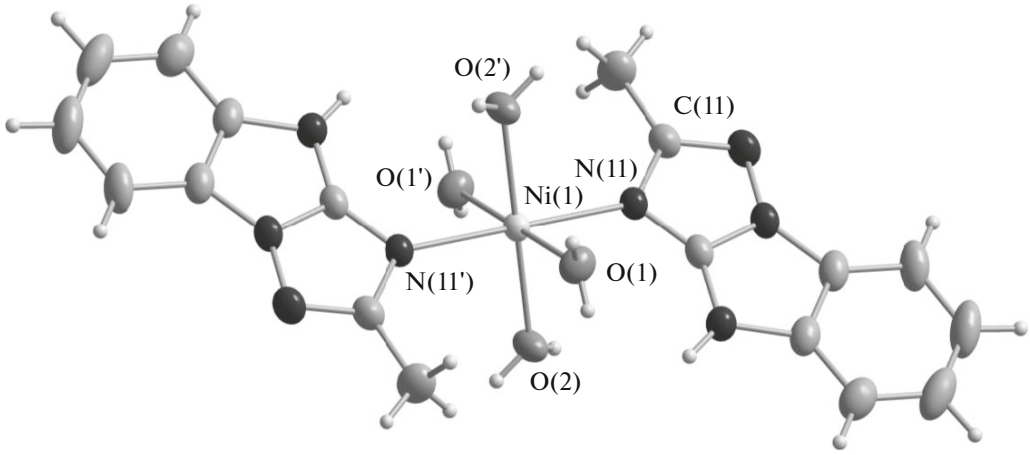

Fig. 2. Structure of complex $[Ni(L)_2(H_2O)_4]Cl_2 \cdot 4H_2O$ (**II**). Atomic shift ellipsoids are presented with 50% probability.

ing or thermal vibrations of the planar ligand. In the structure of complex **II**, on the contrary, the ligand is nearly planar. Thus, the influence of the environment of the ligand on its conformation can be assumed. At the same time, no structurally characterized compounds with the 2-methyl-1,2,4-triazolo[1,5-a]benzimidazole fragment were known up to the present work and, hence, further conclusions about its conformational rigidity are anticipatory.

In three structures, π–π interactions occur between the adjacent L ligands. In the case of compound **IIIa**, intramolecular contacts are observed (the distances between parallel planes of the rings in the dimers with the bromide bridges are 3.0 Å), as well as intermolecular contacts (the distances between parallel planes of the rings are 3.5 Å) due to which the molecules of the complexes are packed in piles along the direction (0 1 0).

In compound **Ia**, ligands L are also arranged in piles but the planes of the rings are not parallel, most likely, because of the steric effect of the chloride ions. The corresponding dihedral angles are 20.9° and, hence, the packing is formed, in this case, due to a more complicated system of contacts involving ligands L and Cl^-. An interesting feature of this structure is the presence of two sorts of symmetrically nonequivalent layers along (1 0 0), which alternate according to the ···AB··· type (Fig. 4). The weak interaction between the

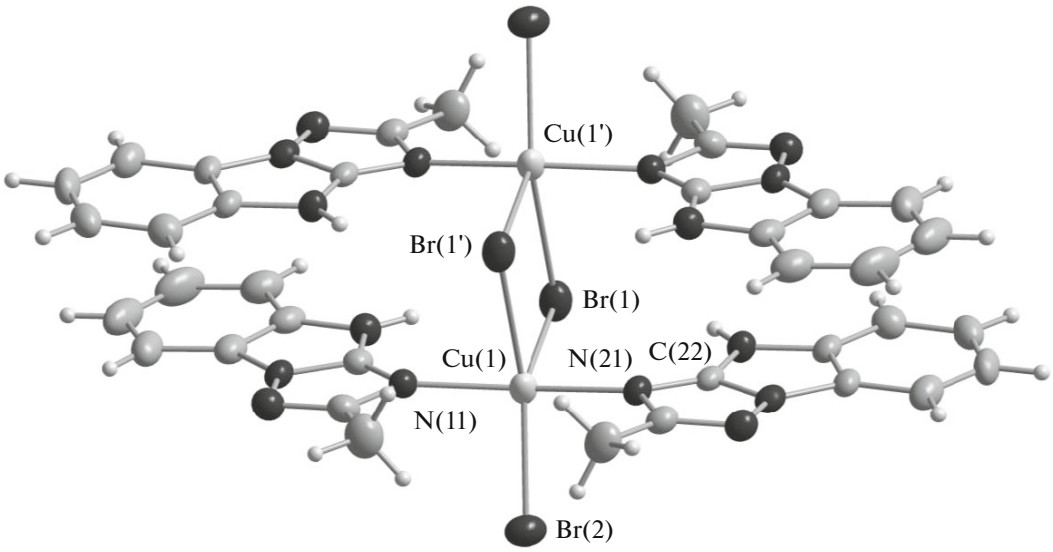

Fig. 3. Structure of complex $[Cu_2(L)_4(\mu\text{-}Br)_2Br_2]$ (**IIIa**). Atomic shift ellipsoids are presented with 50% probability.

layers leads to defects in the packing, which is manifested as a high affinity of the crystals of complex **Ia** to twinning. The structural models obtained for all tested samples with different sizes had significant peaks of the residual electron density (2.7 e/Å^3). The possibility to assign this residual electron density to solvate water is excluded, because the structure is fairly dense and has no "cavities" accessible for the inclusion of solvent molecules. Since no noticeable diffuse scattering is observed for the diffraction patterns, it can be concluded that the size of "ideal" domains is at least tens of the layers (>10 nm). However, these layers are insufficiently frequent for being taken into account by the introduction of the twinning model.

In each complex cation of compound **II**, two ligands contact with the aromatic systems of different cations (the distances between the parallel planes of the rings are 3.1 and 3.6 Å), so that layers are formed along the plane (0 0 1) due to π–π interactions and covalent bonds. Owing to the presence of both coordinated and solvate water molecules, the structure of compound **II** contains hydrogen bonds involving all hydrogen atoms of the water molecules except for one atom (H(3*B*) of the solvate H_2O molecule). Thus, the dimeric layers (Fig. 5) are formed along the plane (1 0 0) due to the OH···O (O···O 2.74 and 2.75 Å) and OH···Cl (O···Cl 3.06–3.17 Å) contacts.

The main vibrational frequencies (cm^{-1}) in the IR spectra of L and three complexes are presented in Table 6. A band at 3404 cm^{-1} and a broad band at 3246 cm^{-1} assigned to the ν(O–H) vibrations are observed in the high-frequency range of the IR spectra of complexes **I** and **II**, respectively, confirming the presence of crystallization (**I** and **II**) and/or inner-sphere (**II**) water molecules in these compounds. The bands caused by the stretching and bending vibrations of the ring sensitive to coordination appear in a range of 1606–1508 cm^{-1}. In the spectra of complexes **I–III**, these bands are shifted predominantly to the low-frequency range relative to the spectrum of L. This pattern characteristic of 3*d*-metal complexes with nitrogen-containing ligands indicates the coordination of

Table 3. Selected bond lengths in complexes **Ia**, **II**, and **IIIa***

Ia		**II**		**IIIa**	
Bond	d, Å	Bond	d, Å	Bond	d, Å
Co(1)–Cl(11)	2.2636(11)	Ni(1)–O(1)	2.0610(13)	Br(1)–Cu(1)	2.6015(8)
Co(1)–Cl(12)	2.2263(13)	Ni(1)–O(2)	2.0462(13)	Br(1)–Cu(1)$^{\#1}$	2.8657(11)
Co(2)–Cl(21)	2.2640(11)	Ni(1)–N(11)	2.1433(14)	Br(2)–Cu(1)	2.4323(9)
Co(2)–Cl(22)	2.2300(12)			Cu(1)–N(11)	1.975(3)
Co(2)–N(21)	2.005(3)			Cu(1)–N(21)	1.969(4)
Co(1)–N(11)	2.006(3)				

* Symmetry codes: $^{\#1}$ $1-x, -y, 1-z$.

Table 4. Selected angles in complexes **Ia**, **II**, and **III**

Ia		**II**		**IIIa**	
Angle	ω, deg	Angle	ω, deg	Angle	ω, deg
Cl(12)Co(1)Cl(11)	113.00(5)	O(1)Ni(1)N(11)$^{\#3}$	88.34(5)	Cu(1)Br(1)Cu(1)$^{\#3}$	88.13(2)
N(11)Co(1)Cl(11)	104.27(7)	O(2)Ni(1)O(1)$^{\#3}$	88.53(6)	Br(1)Cu(1)Br(1)$^{\#3}$	91.87(2)
N(11)Co(1)Cl(12)	112.79(8)	O(2)Ni(1)N(11)$^{\#3}$	94.92(5)	Br(2)Cu(1)Br(1)$^{\#3}$	146.78(3)
N(11)Co(1)N(11)$^{\#1}$	109.05(16)			Br(2)Cu(1)Br(1)	121.34(3)
Cl(22)Co(2)Cl(21)	113.91(5)			N(11)Cu(1)Br(1)	94.94(10)
N(21)Co(2)Cl(21)	104.64(7)			N(11)Cu(1)Br(1)$^{\#3}$	83.98(11)
N(21)Co(2)Cl(22)	112.00(8)			N(11)Cu(1)Br(2)	92.75(10)
N(21)Co(2)N(21)$^{\#2}$	109.13(17)			N(21)Cu(1)Br(1)$^{\#3}$	87.78(11)
				N(21)Cu(1)Br(1)	94.69(10)
				N(21)Cu(1)Br(2)	89.00(11)
				N(21)Cu(1)N(11)	167.51(15)

* Symmetry codes: $^{\#1}$ $-x, y, z$; $^{\#2}$ $1-x, y, z$; $^{\#3}$ $1-x, -y, 1-z$.

Table 5. Parameters of deviation of the ligand geometry from the plane

Complex	Maximum deviations of atoms		Dihedral angles between planes	
	rings {C_6} from plane of ring {C_3N_2}, Å	ring {C_2N_3} from plane of ring {C_3N_2}, Å	rings {C_6} and {C_3N_2}, deg	rings {C_2N_3} and {C_3N_2}, deg
Ia	0.07, 0.04	0.12, 0.15	1.4, 0.8	4.7, 4.3
II	0.02	0.02	1.0	0.8
IIIa	0.05, 0.05	0.12, 0.12	1.4, 2.6	1.4, 3.7

the nitrogen atom of the 1,2,4-triazole cycle to the metal ion, which is consistent with the data of X-ray structure analysis.

The parameters of the diffuse reflectance spectra of the Co(II) and Ni(II) complexes with L are presented in Table 7. Two bands are observed in the spectrum of complex **I**: a broad band at $\nu_1 = 8850$ cm^{-1} and an intense split band at $\nu_2 = 15243-16129$ cm^{-1}. These bands can be attributed to the electron $d-d$ transitions $^4A_2 \rightarrow {}^4T_2(\nu_1)$ and $^4A_2 \rightarrow {}^4T_2(F)(\nu_2)$ in the tetrahedral field of the ligands. Three bands appear in the diffuse reflectance spectra of the $[Ni(L)_2(H_2O)_4]Cl_2 \cdot 4H_2O$

Table 6. Main vibrational frequencies (cm^{-1}) in the IR spectra of L and complexes **I–III**

L	**I**	**II**	**III**	Assignment
	ν, cm^{-1}			
	3404	3246 broad		ν(O–H)
3290	3322	3141	3290	ν(N–H)
3186	3294			
	3208			
3058	2930	2952	2924	ν(C–H)
2991		2857	2852	
2931				
2836				
1598	1606	1597	1605	R_{ring}
1547	1528, 1508	1516	1528	

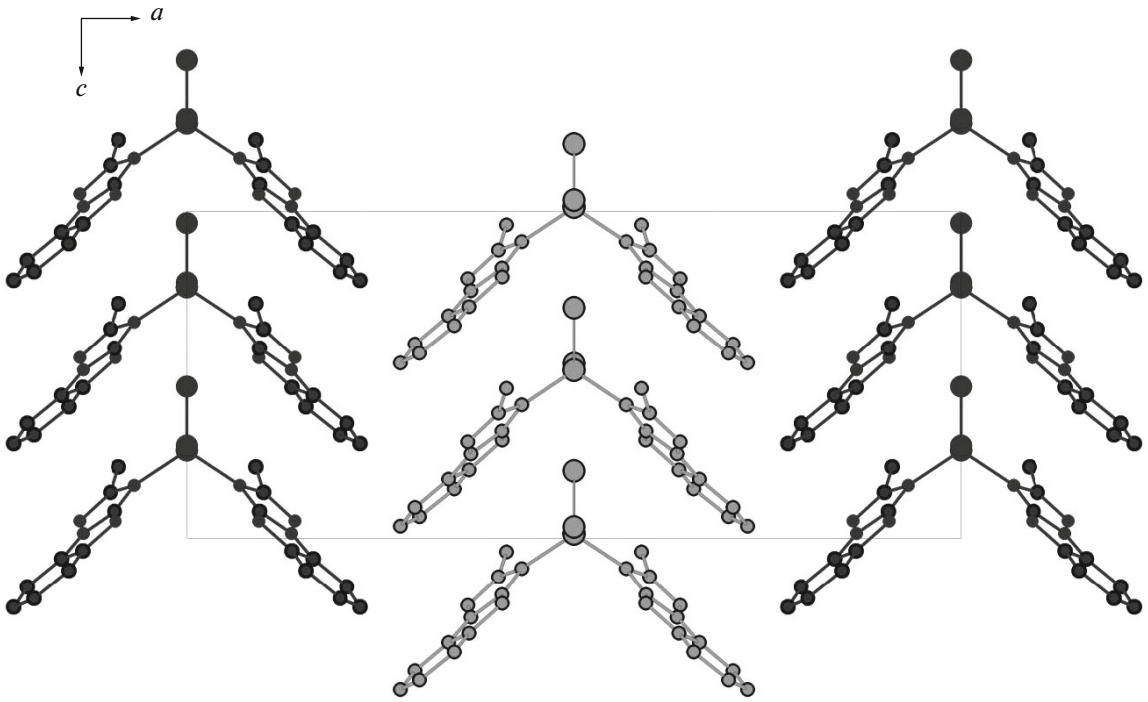

Fig. 4. Packing of molecules of complex **Ia** (crystallographically nonequivalent layers are shown by dark and light).

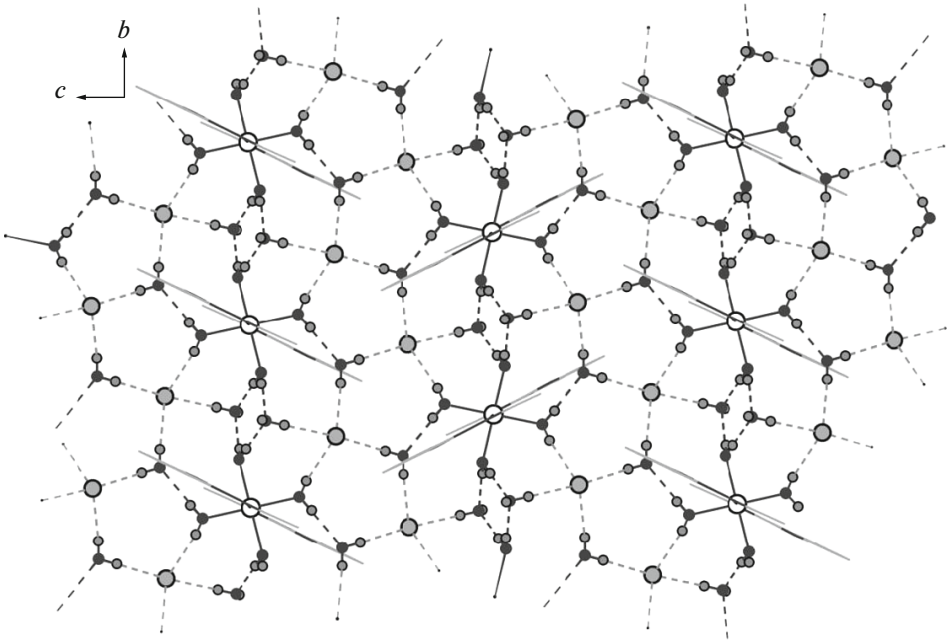

Fig. 5. Structure of the layer formed by hydrogen bonds OH···O and OH···Cl (shown by dash) in the structure of complex **II**.

complex: $\nu_1 = 8333$ cm^{-1}, $\nu_2 = 16447$ cm^{-1}, and $\nu_3 = 26316$ cm^{-1} assigned to the transitions $^3A_{2g} \rightarrow {}^3T_{2g}$, $^3A_{2g} \rightarrow {}^3T_{1g}$, and $^3A_{2g} \rightarrow {}^3T_{1g}(P)$, respectively. This pattern is characteristic of octahedral or pseudo-octahedral Ni(II) complexes with nitrogen-containing ligands. The diffuse reflectance spectrum of complex **III** exhibits one broad band at $\nu_1 = 12077$ cm^{-1}, which can hardly be assigned to a certain electron transition [35].

The study of the cytotoxicity of L and its complexes showed that L, **I**, and **II** exerted no cytotoxic effect in

Table 7. Parameters of the diffuse reflectance spectra for complexes **I** and **II**

Compound	λ_{max}, nm	ν, cm^{-1}	Assignment
$[Co(L^1)_2Cl_2]$ (**I**)	620, 656	16129, 15243	$^4A_2 \rightarrow {}^4T_1(P)$
	1130	8850	$^4A_2 \rightarrow {}^4T_1(F)$
$[Ni(L^1)_2(H_2O)_4]Cl_2 \cdot 4H_2O$ (**II**)	380	26316	$^3A_{2g} \rightarrow {}^3T_{1g}(P)$
	608	16447	$^3A_{2g} \rightarrow {}^3T_{1g}$
	1200	8333	$^3A_{2g} \rightarrow {}^3T_{2g}$

the whole range of the studied concentrations, whereas complex **III** exhibits an appreciable activity (Fig. 6). For this complex, the cell death is observed already at the concentrations >5 μM and reaches a maximum of 80% at 25 μM.

Thus, the complex formation of ligand L with the copper(II) ion is the reason for a substantial cytotoxicity manifested by this complex.

ACKNOWLEDGMENTS

The cytotoxicity of the synthesized compounds was studied using the equipment of the Proteomics Center for Collective Use at the Institute of Molecular Biology and Biophysics of the Federal Research Center of Fundamental and Translational Medicine (Novosibirsk, Russia).

The authors are grateful to N.P. Korotkevich for the detection of diffraction patterns, to N.I. Alferova for recording IR spectra, and to I.V. Yushina for recording electronic spectra.

This work was supported by the Russian Foundation for Basic Research, project no. 16-53-00020 Vel_a.

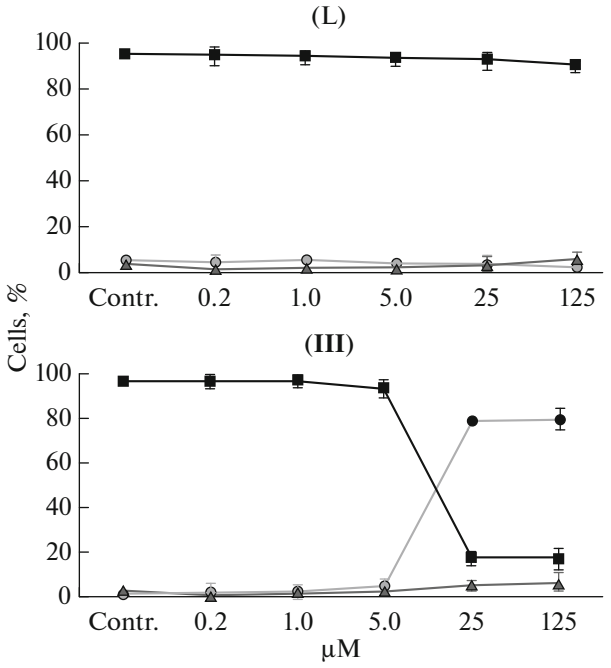

Fig. 6. Cells Hep-2 after 48 h of the treatment with L and complex **III**: contr is control, ■ indicates living cells, ▲ means apoptosis cells, and ● designates dead cells.

REFERENCES

1. Goker, H., Alp, M., and Yildiz, S., *Molecules*, 2005, vol. 10, p. 1377.
2. Iwao, E., Yamamoto, K., Yokoyama, Y., et al., *J. Infect. Chemother.*, 2004, vol. 10, p. 90.
3. Aminabhavi, T.M., Biradar, N.S., and Patil, S.B., *Inorg. Chim. Acta*, 1986, vol. 125, p. 125.
4. Tewari, A.K. and Mishra, A., *Indian J. Chem., B*, 2007, vol. 45, p. 489.
5. Boiani, M. and Gonzalez, M., *J. Med. Chem.*, 2005, vol. 5, p. 409.
6. Mavrova, A.Ts., Wesselinova, D., and Anichina, K., *J. Chem. Technol. Met.*, 2016, vol. 51, p. 660.
7. Akbay, A., Oren, I., Temiz-Arpaci, O., et al., *Arzneim. Forsch.*, 2003, vol. 53, p. 266.
8. Yurdakul, S. and Kurt, M., *J. Mol. Struct.*, 2003, vol. 650, p. 181.
9. Singh, V.P., Katiyar, A., and Singh, S., *J. Coord. Chem.*, 2009, vol. 62, p. 1336.
10. Gumus, F., Algul, O., Eren, G., et al., *Eur. J. Med. Chem.*, 2003, vol. 38, p. 473.
11. Sau, D.K., Butcher, R.J., Chaudhuri, S., and Saha, N., *Mol. Cell. Biochem.*, 2003, vol. 253, p. 21.
12. Mylonas, S., Valavanidis, A., Dimitropoulos, K., et al., *J. Inorg. Biochem.*, 1988, vol. 34, p. 265.
13. Mothilal, K.K., Karunakaran, C., and Rajendran, A., Murugesan, R., *J. Inorg. Biochem.*, 2004, vol. 98, p. 322.
14. Podunavac-Kuzmanovic, S.O. and Cvetcovic, D.M., *J. Serb. Chem. Soc.*, 2007, vol. 72, p. 459.
15. Devereux, M., O'Shea, D., Kellett, A., et al., *J. Inorg. Biochem.*, 2007, vol. 101, p. 881.
16. Paolini, J.P., *Top. Heterocycl. Chem.*, Weissderger, A. and Taylor, E.C., Eds., New York: Intersci., 1977, p. 1.
17. Kuz'menko, V.V., Kuz'menko, T.A., Pozharskii, A.F., et al., *Khim. Geterotsikl. Soedin.*, 1989, vol. 25, no. 2, p. 168.
18. Han, X., Pin, S.S., Burris, K., et al., *Bioorg. Med. Chem. Lett.*, 2005, vol. 15, p. 4029.

19. Anisimova, V.A., Spasov, A.A., Tolpygin, I.E., et al., *Khim.-farm. Zh.*, 2010, vol. 44, no. 7, p. 7.
20. Gütlich, P. and Goodwin, H., *Top Curr. Chem.,* 2004, vol. 233, p. 1.
21. Halcrow, M.A., *Spin-Crossover Materials Properties and Applications*, UK: Wiley, 2013.
22. Lavrenova, L.G. and Shakirova, O.G., *Eur. J. Inorg. Chem.*, 2013, nos. 5–6, p. 670.
23. Kane, J.M., Dudley, M.W., Sorensen, S.M., and Miller, F.P., *J. Med. Chem.*, 1988, vol. 31, p. 1253.
24. Kane, J.M., Baron, B.M., Dudley, M.W., et al., *J. Med. Chem.*, 1990, vol. 33, p. 2772.
25. Kochikyan, T.V., Samvelyan, M.A., Arutyunyan, E.V., et al., *Pharm. Chem. J.*, 2011, vol. 44, p. 525.
26. Matesanz, A.I., Joie, C., and Souza, P., *Dalton Trans.*, 2010, vol. 39, p. 7059.
27. Groessl, M., Reisner, E., Hartinger, C.G., et al., *J. Med. Chem.*, 2007, vol. 50, p. 2185.
28. Bagihalli, G.B., Avaji, P.G., Patil, S.A., and Badami, P.S., *Eur. J. Med. Chem.*, 2008, vol. 43, p. 2639.
29. Groom, C.R., Bruno, I.J., Lightfoot, M.P., and Wards, C., *Acta Crystallogr., Sect. B: Struct. Sci., Cryst. Eng. Mater.*, 2016, vol. 72, p.171.
30. ICSD web version 3.7.0 released. FIZ Karlsruhe, 2017. https://www.fiz-karlsruhe.de.
31. *APEX2 (version 1.08), SAINT (version 7.03), SADABS (version 2.11), SHELXTL (version 6.12)*, Madison: Bruker AXS Inc., 2004.
32. Sheldrick, G.M., *Acta Crystalllogr., Sect. C: Struct. Chem.*, 2015, vol. 71, p. 3.
33. Dolomanov, O.V., Bourhis, L.J., Gildea, R.J., et al., *J. Appl. Crystallogr.*, 2009, vol. 42, p. 339.
34. Lavrenova, L.G., Kuz'menko, T.A., Ivanova, A.D., et al., *New J. Chem.*, 2017, vol. 41, p. 4341.
35. Lever, A.B.P., *Inorganic Electronic Spectroscopy*, Amsterdam: Elsevier, 1987.

Translated by E. Yablonskaya